XAFS studies of monodisperse Au nanoclusters formation in the etching process

Lina Yang, Ting Huang, Wei Liu, Jie Bao, Yuanyuan Huang, Yuanjie Cao, Tao Yao, Zhihu Sun*, and Shiqiang Wei*

National Synchrotron Radiation Laboratory, University of Science and Technology of China, Hefei, Anhui 230029, P. R. China

Corresponding authors. E-mail: zhsun@ustc.edu.cn, sqwei@ustc.edu.cn

Abstract. Understanding the formation mechanism of gold nanoclusters is essential to the development of their synthetic chemistry. Here, by using x-ray absorption fine-structure (XAFS) spectroscopy, UV-Vis and MS spectra, the formation process of monodisperse Au_{13} nanoclusters is investigated. We find that a critical step involving the formation of smaller Au_8–Au_{11} metastable intermediate clusters induced by the HCl + HSR etching of the polydisperse Au_n precursor clusters occurs firstly. Then these intermediate species undergo a size-growth to Au_{13} cores, followed by a slow structure rearrangement to reach the final stable structure. This work enriches the understanding of cluster formation chemistry and may guide the way towards the design and the controllable synthesis of nanoclusters.

1. Introduction

Gold nanoclusters possess size-dependent molecular-like structure and discrete electronic energy levels, which render them diverse applications in fields such as catalysis, optical devices and imaging [1-5]. Therefore, the development of synthetic strategies for monodisperse Au nanoclusters is crucial. Currently, etching polydisperse Au clusters has been widely employed as an useful top-down method and obtained remarkable advances. However, the mechanistic understanding on the etching-induced synthesis of monodisperse nanoclusters is still to be resolved [6]. Therefore, it is important to study etching reactions for developing more routes to fine-tune nanoclusters with desired functionalization.

Currently, direct liberation of the same-sized particle as the target cluster in a single step was hypothesized but not experimentally verified [7]. What happens in the convergence process and how this process is related to the structure and property of the end product is scarcely known. In order to solve these problems, in-situ methods by a combination of various probing techniques with sensibility to transient intermediate species in solution are specially required.

Herein, we report an investigation on the kinetic formation process of an unprecedented monodisperse $Au_{13}(L_3)_2(SR)_4Cl_4$ nanocluster (L_3: 1,3-Bis(diphenylphosphino)propane) by in-situ x-ray absorption fine structure (XAFS), UV-vis absorption and MS spectra. The Au_{13} nanocluster is obtained via a facile one-phase reaction of polydisperse Au_n clusters with hydrochloric acid (HCl) and dodecanethiol (HSR). It is found that the formation of the monodisperse $Au_{13}(L_3)_2(SR)_4Cl_4$ nanoclusters is realized in an etching/growth/rearrangement manner including three reaction stages.

2. Experimental Section

Sample preparations: The monodisperse Au nanoclusters were synthesized by reaction of HCl and HSR mixture with preformed L_3-capped Au_n clusters. The starting material of this reaction, L_3-capped Au_n clusters, was synthesized by reduction of $Au_2(L_3)Cl_2$ (70 mg, 0.08 mmol) with $NaBH_4$ (15 mg, 0.04 mmol) in 60 ml dichloromethane solvent at room temperature for 3 h under stirring [6]. The solvent was evaporated to dryness and then redissolved in 12 ml ethanol, to which a mixture of dodecanethiol (50 μL, 0.2 mmol) and HCl (200 μL, 2.4 mmol) was added. The process of the reaction was monitored by in-situ XAFS spectra, UV-Vis, as well as mass spectrometry.

In-situ XAFS measurement: The Au L_3-edge XAFS spectra were measured at the BL14W1 beamline of the Shanghai Synchrotron Radiation Facility (SSRF). The storage ring of SSRF worked at 3.5 GeV with a maximum current of 210 mA. The reactive solution was continuously circulated along a microtube by peristaltic pump and flowed into an in-situ cell for XAFS measurement.

3. Results and discussion

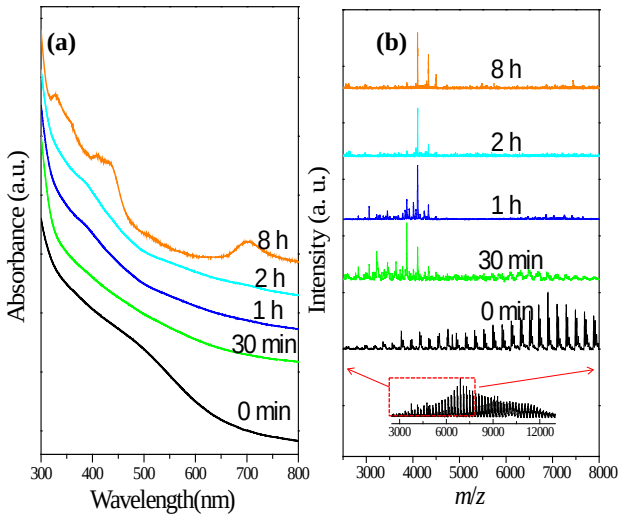

Figure 1. *In situ* UV-vis absorption spectra and MALDI mass spectra at different reaction times. The inset shows the MALDI-MS of the starting material at a wide mass range.

The time-dependent UV-vis absorption and MALDI-MS spectra for the formation process of monodisperse $Au_{13}(L_3)_2(SR)_4Cl_4$ nanoclusters were shown in Fig. 1. At first, the UV-Vis spectrum demonstrates a wide hump at around 500 nm, suggesting the polydispersity of the precursor clusters.

At 30 min the spectral profile shows a featureless decay. From 2 h on, absorption bands peaked at 327, 410, 433, and 700 nm become gradually pronounced and reach saturation. The MS spectra for the starting material covers a wide size range of 3000–13000 Da, corresponding to a mixture of Au_{15}–Au_{60}. Within the 30 min, the wide size distribution is divided into two regions covering roughly 6000–8000 and 3000–4000 Da, which could be assigned to Au_{31}–Au_{39} and Au_8–Au_{11} clusters respectively. At 2 h, only the peaks at 4101 and 4335 Da are present. These two peaks are corresponding to $Au_{13}(L_3)_2(SR)_4Cl_4$ cluster (a fragment of and intact, respectively), indicating complete size-convergence into Au_{13} clusters.

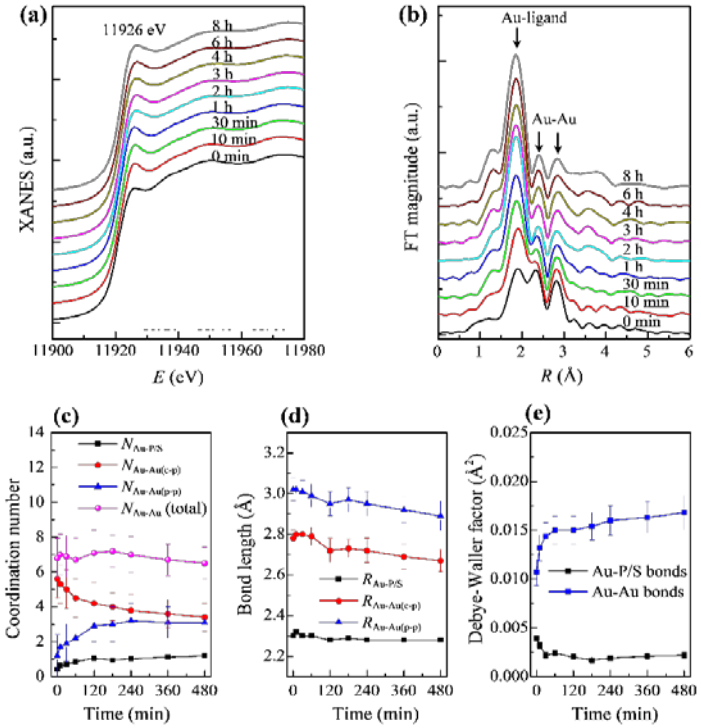

Figure 2. (a) Time-dependent XANES spectra, and (b) EXAFS spectra. (c) Coordination number CN, (d) bond distance *R*, and (e) Debye-Waller factor σ^2 against reaction time extracted from EXAFS curve-fitting. Au–Au(c-p) and Au–Au(p-p) represent the central-peripheral and peripheral-peripheral Au–Au bonds in an complete or incomplete icosahedron, respectively.

In situ XAFS measurements at Au L_3-edge were performed to detect the evolutions of the size-conversion process. The XANES spectra in Fig. 2(a) display that the spectrum of the starting material exhibits a peak at 11936 eV (labeled by an arrow), which is characteristic of fcc structured Au. After addition of HCl + HSR, the intensity of this peak is remarkably smeared out at 30 min, and disappears completely at 2h. The peak shape is similar to nanoclusters. The Fourier transformed (FT) EXAFS $k^2\chi(k)$ curves in Fig. 2(b) also show that immediately after the start of reaction (within 30 min), the Au-ligand (Au−S/P/Cl) peak at 1.90 Å is intensified rapidly, while the Au-Au peaks (2.36 and 2.88 Å) are significantly damped, suggesting the decomposition of the larger clusters. Moreover, the white-line peak at around 11926 eV in the XANES spectrum, corresponding to the $2p_{3/2}\rightarrow 5d_{5/2,3/2}$

electronic transition of Au atoms, is significantly intensified immediately after the addition of HCl + HSR. With continued reaction, the white-line peak is reduced slightly in intensity, along with the gradually weakened Au-Au peaks in the FT curve. After 2 h, the XANES spectra do not display any remarkable changes, while subtle continuing increase of the Au-ligand EXAFS peak intensity could be discerned .Quantitative structural parameters have been obtained through a least-squares curve-fitting using the ARTEMIS [8] module of IFEFFIT package. We will discuss the details in the following.

Within the first stage of 30 min, Au_{15}–Au_{60} clusters with Au-ligand CN of 0.44, are prominently etched into smaller Au_8–Au_{11} metastable intermediates. Subsequently, these active small Au_8–Au_{11} clusters are immediately stabilized by the absorbed SR, L_3 and Cl^- ligands to form metastable intermediates as evidenced by the quickly increased Au-ligand CN (from 0.44 at 0 min to 0.72 at 30 min). These Au_8–Au_{11} cores are fully protected by the ligands, forming closed geometrical shells that make the clusters highly resistant against etching. In the second stage (30 min-2 h), these metastable Au_8–Au_{11} intermediates focus into Au_{13} cores, which is possibly achieved by incorporating the Au(I) ions or Au(I)-Cl oligomers pre-existing in the solution. The obtained Au-ligand CN (1.02) at 2h is between the nominal values in $Au_{13}(L_3)_2(SR)_4Cl_4$ (0.92) and Au(I)-SR polymers (2.0) [10], suggesting the existence of both species. The proportion p of the Au atoms in $Au_{13}(L_3)_2(SR)_4Cl_4$ could be estimated by the equation $0.92\times p+2\times(1-p)=1.02$, which gives $p\sim0.90$. This result demonstrate that the majority (~90%) of Au atoms at 2 h is in the form of Au_{13} cluster, with a small part (~10%) forming Au(I)-SR polymers or analogues. In the third stage (after 2 h), the atomic structure undergoes a rearrangement process toward the energetically stable structure. The EXAFS curve-fitting show that during the structure rearrangement process, the Au–Au bond displays a trend of contraction. At the beginning of forming Au_{13} skeletons, both the $R_{Au\text{-}Au(c\text{-}p)}$ and $R_{Au\text{-}Au(p\text{-}p)}$ (2.72 and 2.95 Å) of the Au_{13} icosahedron are within the typical range (2.71–2.79 and 2.85–2.95 Å) of Au_{13} clusters as previously reported [9]. After the structure rearrangement, the $R_{Au\text{-}Au(c\text{-}p)}$ and $R_{Au\text{-}Au(p\text{-}p)}$ decrease to 2.67 and 2.89 Å, respectively, suggesting a considerable structural distortion away from the original icosahedral Au_{13} skeleton. The gradually enlarged distortion is also reflected by the slightly increased disorder degree σ^2 of the Au-Au bonds, from 0.015 to 0.017 $Å^2$. This implies the structural rearrangement of Au_{13} clusters.

4. Conclusion

In summary, in-situ XAFS combined with MS and UV-Vis have been used to probe the formation process of the monodisperse $Au_{13}(L_3)_2(SR)_4Cl_4$ nanocluster. It is found that the cluster formation is achieved in an etching/growth/rearrangement manner including three distinct reaction steps. (1) The initial polydisperse Au_n clusters are etched to form much smaller Au_8–Au_{11} intermediate clusters. (2) These intermediate species undergo a size growth to Au_{13} cores, by incorporating the pre-existing Au(I) ions or Au(I)-Cl oligomers in the solution. (3) Finally, a slow structure rearrangement of the Au_{13} skeleton and the covering ligand shells occurs. These findings enrich our understanding on the etching mechanism and can guide our way towards the synthesis of nanomaterials in a controllable manner.

Acknowledgments

This work was supported by National Natural Science Foundation of China (Grant No. 11475176, 11135008, U1332131, and 11305172). The authors are grateful to SSRF for the valuable beamtime.

References

[1] Jin, R. C. *Nanoscale* 2010, 2, 343.
[2] Li, G.; Jin, R. C. *Acc. Chem. Res.* 2013, 46, 1749.
[3] Qian, H. F.; Zhu, M. Z.; Wu, Z. K.; Jin, R. C. *Acc. Chem. Res.* 2012, 45, 1470.
[4] Yau, S. H.; Varnavski, O.; Goodson, T. *Acc. Chem. Res.* 2013, 46, 1506.
[5] Lu, Y. Z.; Chen, W. *Chem. Soc. Rev.* 2012, 41, 3594.
[6] Shichibu, Y.; Konishi, K. *Small* 2010, *6*, 1216.
[7] Duan, H. W.; Nie, S. M. *J. Am. Chem. Soc.* 2007, *129*, 2412.
[8] Ravel, B.; Newville, M. *J. Synchrotron Rad.* 2005, *12*, 537.
[9] Hall, K. P.; Mingos, D. M. P. *Prog. Inorg. Chem.* 1984, *32*, 237.
[10] Menard, L. D.; Frenkel, A. I.; Murray, R. W.; Nuzzo, R. G. *J. Phys. Chem. B* 2006, *110*, 14564.